Proceedings of the World Congress on Mechanical, Chemical, and Material Engineering (MCM 2015)
Barcelona, Spain – July 20 - 21, 2015
Paper No. 328

Analysis of Shock-plugs in Quasi-One-Dimensional Compressible Flow

Thomas Adams, Eric Chang, Benjamin Stevens, Matthew Thompson
Rose-Hulman Institute of Technology
5500 Wabash Ave, Terre Haute, IN 47803, USA
adams1@rose-hulman.edu; changet@rose-hulman.edu; stevenbc@rose-hulman.edu; thompsm2@rose-hulman.edu

Abstract **-**With the continuing miniaturization of technology happening a rapid pace, more and more compressible flows are occurring at the microscale. At the small length scales encountered in such microflows, the standard assumption of shockwaves having infinitesimal thickness may no longer apply. In this paper we therefore suggest the existence of "shock-plugs," standing normal shocks with finite thickness. We model shock-plugs using the same methods and assumptions as seen in standard normal shockwave analysis. The inclusion of shock thickness necessitates the inclusion of additional parameters in the analysis, however, namely differing upstream and downstream cross sectional areas, as well the pressure on the sidewalls adjacent to the shock. Predictions for changes in Mach number, temperature, pressure, and entropy are presented, all of which show deviation from conventional shockwave analysis. The models presented here may provide better estimates of shock properties in microscale applications.

Keywords**:** shock-plug, shockwave, compressible flow, microflows, microfluidics

1. Introduction

In the quasi-one-dimensional flow of a compressible fluid in a converging/diverging nozzle, the fluid can be accelerated from subsonic flow in the converging section to supersonic flow in the diverging section if a suitably low back pressure exists. For isentropic flow, one unique value of back pressure will produce a constantly accelerated flow throughout the channel such that the value of back pressure exactly matches the pressure at the exit as required by isentropic conditions. For back pressures larger than this, however, isentropic flow cannot be maintained throughout, and a normal shockwave forms in the diverging section. (Fig. 1.) The upstream and downstream isentropic flows are effectively pieced together via the shockwave. (Moran and Shapiro, 2008)

Modelling of shockwaves is well developed and relies on the application of continuity, linear momentum conservation, and energy conservation across an infinitesimally thin control volume. The presence of the shockwave rapidly decelerates the flow from supersonic to subsonic conditions, causing a discontinuous increase in pressure accompanied by a large generation of entropy. Good treatments can be found in Anderson (1990) and NACA (1953).

The simple relations that result from the standard analysis of normal shockwaves hinge on the assumption of their infinitesimal size. Anderson (1990) notes that the actual size of shocks is on the order of several mean free paths of the fluid molecules, making the negligible thickness assumption a more than plausible assumption in the vast majority of applications. Granger (1995) gives a quantitative analysis on the size of shockwaves, the basis for which is the balance between viscous shear stress fluid deceleration. The resulting shockwave thickness given by

$$t_{shock} = \frac{\nu}{C_x Ma_x}, \tag{1}$$

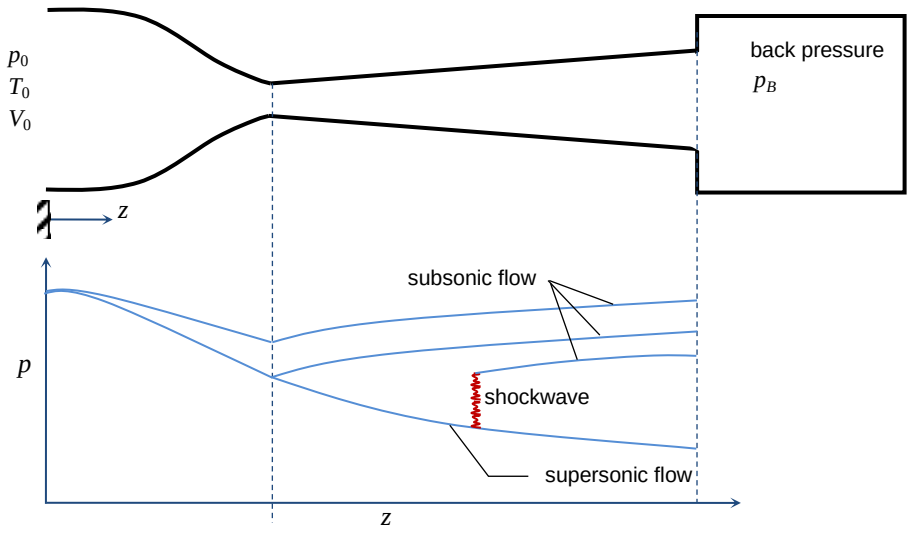

Fig. 1. A converging/diverging nozzle. For sufficiently low back pressures, supersonic conditions can exist in the diverging portion. For a certain range of back pressures, shockwaves form, across which the flow decelerates from supersonic to subsonic speeds.

where v is kinematic viscosity, and C_x and Ma_x are the speed of sound and Mach number upstream of the shock, respectively. For air at ambient conditions, this gives values of t_{shock} on the order of 30 nm, well within reason for assuming zero shockwave thickness.

Compressible flow in microfluidic applications, such as shock tubes within microchannels (Iancu and Müller, 2005; Zeitoun et al, 2009; Dodulad et al, 2010) and the design of micronozzles (Louisos et al, 2008), however, involve length scales in which shockwave thickness may potentially be of interest. Specifically, in the case a converging/diverging micronozzle, a finite shockwave thickness may result in non-negligible differences in cross sectional flow areas upstream and downstream of the shock itself, a situation in which standard relations would no longer apply. To the authors' knowledge no analysis currently exists in which shock relations take shock thickness into account. A first order analysis of such hypothesized finite-sized standing shocks, hereafter referred to as "shock-plugs," forms the basis of this paper.

2. Model Derivation

Figure 2 gives a diagram of a standard standing normal shockwave next to the hypothesized shock-plug. In both cases the shock would appear in the diverging section of a converging/diverging nozzle, with supersonic conditions upstream of the shock and subsonic conditions downstream. Variables describing conditions upstream are denoted with x-subscripts, whereas downstream parameters utilize y-subscripts.

The application of continuity, conservation of linear momentum, and conservation of energy to the shockwave in Fig. 2 (a), along with the assumption of a perfect ideal gas, results in the well-known normal shock relations. In these relations, the upstream supersonic Mach number Ma_x completely determines the downstream subsonic Mach number Ma_y, as well as the corresponding increases in temperature, pressure, and density across the shock. Key to the shock functions' dependence only on Ma_x is the shockwave's assumed thinness, which necessarily implies the upstream and downstream flow areas be the same.

The shock-plug shown in Fig. 2 (b), however, is characterized by some thickness, t_{shock}, resulting in the cross sectional area increasing in the flow direction. Also seen in Fig. 2 (b) is the presence of a pressure on the sidewalls of the nozzle, p_{side}, which contributes to the flow direction linear momentum differently than in a shockwave. For the analysis here, the ratio of areas is given the symbol r:

$$r = A_x/A_y. \tag{2}$$

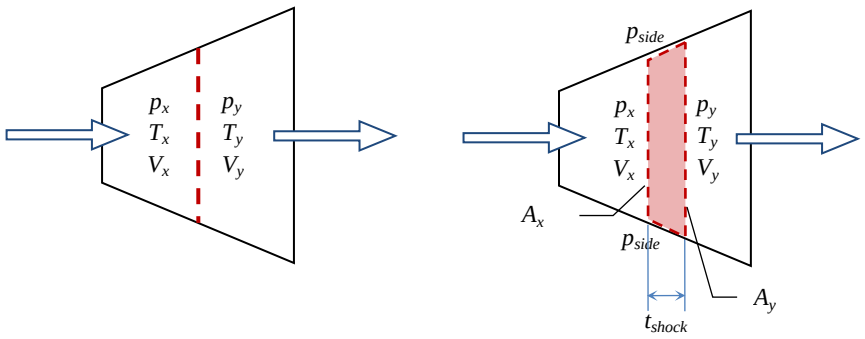

(a) (b)

Fig. 2. Schematic diagrams showing relevant parameters for (a) a shockwave and (b) a shock-plug

The average pressure on the sidewalls is assumed to take on some value between p_x and p_y as given by

$$p_{side} = p_x + \phi\,(p_y - p_x), \tag{3}$$

where $0 < \phi < 1$. The presence of the additional parameters r and ϕ complicates the relations for shock-plugs.

As a first order approximation for estimating the change of parameters across a finite-sized normal shock, we employ the same assumptions used in the derivation of standard normal shock relations, save the exceptions already given. Namely, these include quasi-one-dimensional flow (flow parameters varying only in the stream-wise direction), adiabatic flow, no wall friction, and the use of the perfect ideal gas model as the basis for physical and thermal equations of state. It should also be noted that a known nozzle geometry (that is, a known variation of cross sectional area with flow direction) along with a given value of t_{shock} completely determine the value of r at a given location. As such, in the present analysis we will treat r as an independent variable, removing the need for both detailed knowledge about channel geometry as well as estimates of shock thickness such as that given in Eq. 1.

With these assumptions, the application of continuity across the shock-plug of Fig. 2 (b) gives

$$\rho_x A_x V_x = \rho_y A_y V_y. \tag{4}$$

For an ideal gas the density is $\rho = p/RT$, and the speed of sound is given by $C = \sqrt{\gamma RT}$. Substituting into Eq. (4),

$$\frac{p_x A_x V_x}{C_x^2} = \frac{p_y A_y V_y}{C_y^2}. \tag{5}$$

Recognizing V/C as Mach number, and employing $C = \sqrt{\gamma RT}$ once again, this becomes

$$\frac{Ma_y}{Ma_x} = \frac{A_x}{A_y}\frac{p_x}{p_y}\left(\frac{T_y}{T_x}\right)^{1/2} = r\frac{p_x}{p_y}\left(\frac{T_y}{T_x}\right)^{1/2}. \tag{6}$$

The pressure ratio and temperature ratio in Eq. (6) are found by the applications of conservation of linear momentum and conservation of energy, respectively.

Linear momentum in the flow direction gives

$$p_x A_x + p_{side}(A_y - A_x) + \rho_x A_x V_x^2 = p_y A_y + \rho_y A_y V_y^2. \tag{7}$$

We once again use the ideal gas relations for ρ and C along with the definition of Mach number, and also incorporate the relation given in Eq. (3) for p_{side}. After much manipulation this results in

$$\frac{p_y}{p_x} = \frac{\left(1+\gamma Ma_x^2\right)r + (1-\phi)(1-r)}{\left(1+\gamma Ma_y^2\right) - \phi(1-r)}. \tag{8}$$

Energy conservation across the shock-plug yields

$$h_x + \frac{V_x^2}{2} = h_y + \frac{V_y^2}{2} = \text{constant} \equiv h_0, \tag{9}$$

where h is enthalpy. Equation (9) also shows that the stagnation enthalpy h_0, the resulting enthalpy if the fluid were brought to zero velocity, remains constant across the shock-plug. Substituting c_pT for enthalpy as well as incorporating relations for ρ, C and Ma as before, Eq. (9) eventually yields

$$\frac{T_y}{T_x} = \frac{1 + Ma_x^2 \dfrac{\gamma - 1}{2}}{1 + Ma_y^2 \dfrac{\gamma - 1}{2}}. \tag{10}$$

Together Eqs. (6), (8), and (10) form the counterparts of the normal shock relations for a shock-plug. The reader may notice that the form of Eq. (10) is identical for both shockwaves and shock-plugs. This is because the form of conservation of energy resulting here depends on the shock being modelled as adiabatic, and is thus independent of shock thickness *per se*. Equations (6) and (8) reduce to normal shockwave relations as the area ratio r approaches one.

The application of the second law of thermodynamics shows that the flow across a shock is irreversible with an entropy generation per unit mass being equal to the increase in entropy across it:

$$s_{gen} = s_y - s_x = c_p \ln(T_y / T_x) - R \ln(p_y / p_x). \tag{11}$$

Given that stagnation properties reflect the values of properties if the flow were brought to zero velocity isentropically, and that the stagnation temperature does not increase across a shock, the entropy generation can be expressed solely as a function of the decrease in stagnation pressure:

$$s_{gen} = s_y - s_x = -R \ln(p_{0,y} / p_{x,0}). \tag{12}$$

As is the case with the application of conservation of energy, the form of the relation for entropy increase is identical for a shockwave and a shock-plug.

3. Results and Discussion

Equations (6), (8), and (10) can be combined to eliminate pressure and temperature in order to find a relation between Ma_y and Ma_x. The result is

$$Ma_y = \left[\frac{K_1\gamma(1-K_2)-1 \pm \left(1-2K_1\gamma(1-K_2)+K_1(\gamma-1)(1-K_2)^2\right)^{1/2}}{\gamma-1-K_1\gamma^2} \right]^{1/2}, \tag{13}$$

where

$$K_1 = \frac{Ma_x^2 r^2 \left(2+Ma_x^2(\gamma-1)\right)}{\left((1+\gamma Ma_x^2)r+(1-\phi)(1-r)\right)^2} \tag{14}$$

and

$$K_2 = \phi(1 - r)\ . \tag{15}$$

The "minus" solution in Eq. (13) corresponds to a supersonic Ma_y in which the fluid continues to accelerate through the plug, whereas the "plus" solution corresponds to the subsonic, shock-plug solution for Ma_y.

Figure 3 shows the variation of Ma_y with Ma_x as calculated by Eq. (13) for various values of r. In all cases ϕ is set to 0.5 so that p_{side} is the arithmetic average of p_x and p_y.

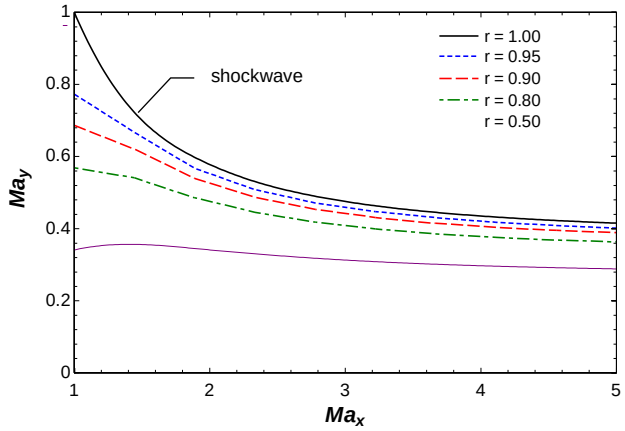

Fig. 3. Variation of downstream Mach number for various area ratios

It is evident from Fig. 3 that the larger the difference in area between shock-plug inlet and outlet (smaller r), the more the shock-plug solution deviates from the standard normal shock values. The effect is most pronounced at smaller Ma_x, with Ma_y becoming a function only of r at high Ma_x.

Figures 4 (a) and (b) show the pressure and temperature increases across the shock-plug, respectively. The ranges of Ma_x and r are the same as in Fig. 3. From Fig. 4 (a) we see that pressure increases less across shock-plugs compared to shockwaves, whereas Fig. 4 (b) shows that temperature increases more. As is the case with Ma_y, smaller area ratio results in more deviation from shockwave behaviour for both pressure and temperature. As opposed to Ma_y, which shows more deviation from shockwave behaviour at lower Ma_x, pressure shows more deviation at higher Ma_x. The deviation in temperature compared to shockwaves is small, and does not show any clear trend with Ma_x.

In Fig. 5 can be seen the entropy generation for the same range of parameters as in the previous comparisons. Shock-plugs clearly result larger entropy generation, and therefore more irreversibility than do shockwaves. This trend continues with larger changes in area for all Mach numbers.

The irreversibility in shockwaves is often attributed to friction and conduction heat transfer within the shock itself. (Anderson, 1990) Given that the modelling equations are written assuming an adiabatic process with no accounting of wall friction, however, coupled with the assumption of an infinitesimally

thin shockwave, we may have reason to question this explanation. Germane to this discussion is the fact that the form of Eq. (12) for entropy generation is exactly the same as for an ideal gas undergoing an unrestrained, adiabatic expansion in what would otherwise be a quasistatic process. Seeing as how shock-plugs occur over finite volumes, and that Fig. 5 shows larger irreversibilities for larger changes in area, we may wonder if the source of entropy generation in shocks is not better thought of as the result of the total pressure of a gas decreasing as it "expands against nothing," more expansion leading to more irreversibility.

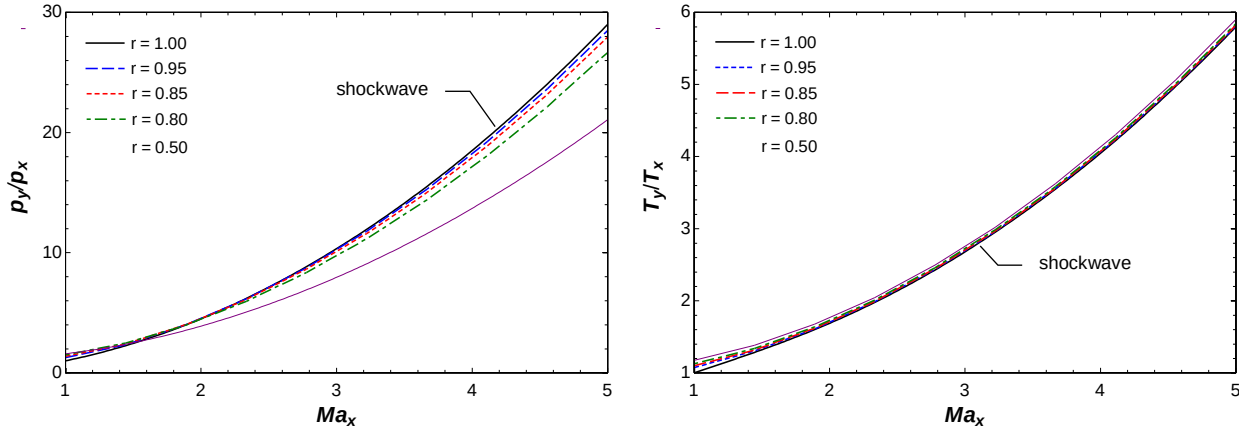

(a) (b)

Fig. 4. (a) Pressure increase and (b) temperature increase across shock-plugs of various area ratios

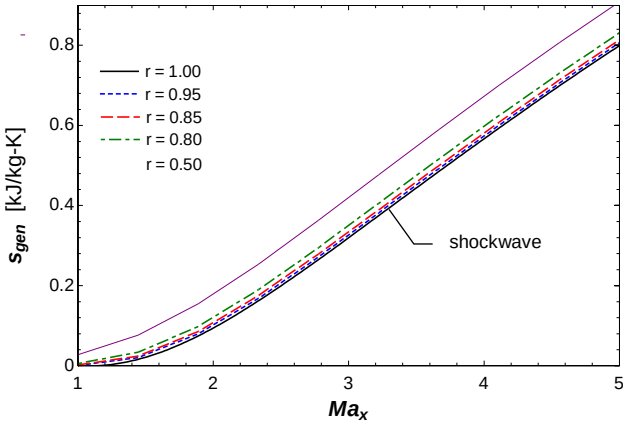

Fig. 5. Entropy generation per unit mass

Furthermore, the estimate for shock thickness given by Eq. 1 may also be called into question in that it balances pressure against viscous shear stress, yet it employs the values of pressure found from standard shock relations, which, as previously noted, ignore wall shear stress. Modelling a shock-plug as an unrestrained expansion may therefore also have value in providing better estimates for shock thickness. This remains a topic for future work.

The effects of varying values of the average pressure on the walls of the channel, $p_{side,}$ via changing ϕ are not explored in this preliminary study. Naturally questions arise as to the appropriate value of ϕ and its functional dependence. This too is left for future investigations.

4. Conclusion

In this paper we have hypothesized the existence of and subsequently modelled shock-plugs, standing normal shocks of finite thickness. In shock-plugs the assumption of finite thickness requires analysis to include different upstream and downstream cross sectional areas, as well as an average pressure on the

sidewalls of the shock. The inclusion of these extra variables complicates the analysis of property changes across the shock, resulting in larger changes in Mach number accompanied by smaller pressure increases, larger temperature increases, and larger entropy increases. The analysis of shock-plugs also suggests that the entropy generation across shocks may best be visualized as a form of unrestrained expansion. The models presented here may provide better estimates of shock properties in applications with very small length scales, in which the thickness of shocks may not necessarily be negligible.

Acknowledgements

The authors wish to thank ArcelorMittal and the Rose-Hulman Institute of Technology Independent Project/Research Opportunities Program for their support in this work.

References

Ames Research Staff (1953). Equations, Tables, and Charts for Compressible Flow, *Report 1135, National Advisory Committee for Aeronautics (NACA).*

Anderson, J.D. (1990). Modern Compressible Flow With Historical Perspective. McGraw-Hill.

Doduladab, O.I., Klossa, Y.Y., Tcheremissinebc, F.G., & Shuvalov, P.V. (2010). Simulation Of Shock Wave Propagation In A Microchannel By Solving The Boltzmann Equation. *Matem. Mod.*, 22 (6), 99–110.

Granger, R.A. (1995). Fluid Mechanics. Dover.

Iancu, F., & Müller, N. (2005). Efficiency Of Shock Wave Compression In A Microchannel. *Microfluid Nanofluid*, Springer-Verlag.

Louisos, W.F., Alexeenko, A.A., Hitt, D.L., &Zilic, A. (2008). Design Considerations For Supersonic Micronozzles. *International Journal of Manufacturing Research*, 3(1), 80 – 113.

Moran, M.J., & Shapiro, H.N. (2008). Fundamentals of Engineering Thermodynamics 6th edition. Wiley.

Zeitoun, D.E., Graur, I.A., Burtschell, Y., Ivanov, M.S., Kudrayvstev, A.N., & Bondar, Y.E. (2009). Continuum and Kinetic Simulation of Shock Wave Propagation in Long Micrcochannel. *Proc. of Rarefied Gas Dynamics: 26th Int. Symposium*, 464-469.